ELSEVIER

Engineering Geology 58 (2000) 231–249

ENGINEERING GEOLOGY

www.elsevier.nl/locate/enggeo

Statistical analysis of an earthquake-induced landslide distribution — the 1989 Loma Prieta, California event

David K. Keefer *

US Geological Survey, Menlo Park, CA 94025, USA

Received 17 December 1998; accepted for publication 21 February 2000

Abstract

The 1989 Loma Prieta, California earthquake (moment magnitude, **M** = 6.9) generated landslides throughout an area of about 15,000 km^2 in central California. Most of these landslides occurred in an area of about 2000 km^2 in the mountainous terrain around the epicenter, where they were mapped during field investigations immediately following the earthquake. The distribution of these landslides is investigated statistically, using regression and one-way analysis of variance (ANOVA) techniques to determine how the occurrence of landslides correlates with distance from the earthquake source, slope steepness, and rock type. The landslide concentration (defined as the number of landslide sources per unit area) has a strong inverse correlation with distance from the earthquake source and a strong positive correlation with slope steepness. The landslide concentration differs substantially among the various geologic units in the area. The differences correlate to some degree with differences in lithology and degree of induration, but this correlation is less clear, suggesting a more complex relationship between landslide occurrence and rock properties.

Keywords: California; Earthquake; Landslide; Loma Prieta; Statistical analysis

1. Introduction

Earthquake shaking is one of the main agents of landslide generation, with the largest earthquakes capable of triggering thousands of landslides throughout areas of more than 100,000 km^2 (Keefer, 1984a). Such landslides can cause considerable damage and loss of life. For example, landslides caused more than 50% of the economic losses in the great 1964 earthquake in Alaska (moment magnitude, **M** = 9.2; Keefer, 1984a) and killed more than 120,000 people during an **M** = 7.8 earthquake in China in 1920 (Wang and Xu, 1984). Understanding where such landslides are most likely to occur is important for reducing damage and loss of life in future earthquakes. This paper presents a statistical analysis of the distribution of landslides triggered by one well-documented recent earthquake — the 1989 Loma Prieta, California event (**M** = 6.9) — as part of the effort to add to this understanding.

The analysis relates the landslide concentration (LC) — expressed as the number of landslide sources per square kilometer of surface area — to three observable factors that are typically recorded during comprehensive post-earthquake field investigations and that relate to the physical parameters that control the seismic stability of slopes. These three observable factors are distance from the earthquake source, which is related to the strength

* Fax: +1-650-3295163.
E-mail address: dkeefer@usgs.gov (D.K. Keefer)

0013-7952/00/$ - see front matter
PII: S0013-7952(00)00037-5

of shaking, slope steepness, which is related to shear stress, and rock type, which is related to material strength.

The general correlation of landslide occurrence with slope steepness, distance from the earthquake source, and rock type has been observed after many earthquakes (see summaries by Keefer, 1984a,b, 1993, 1999; Wilson and Keefer, 1985; Keefer and Wilson, 1989; Hansen and Franks, 1991), and two previous studies have analyzed landslide distributions using statistical methods to determine whether the landslides resulted from earthquakes that had occurred several decades earlier (Simonett, 1967; Jibson, 1985; Jibson and Keefer, 1989). Both studies concluded that the clustering of landslides around likely earthquake sources indicated that the landslides were seismically triggered. The Loma Prieta earthquake provided an opportunity for statistical analysis of a landslide distribution known to have been produced by an earthquake. The present analysis is similar to those described by Simonett (1967), Jibson (1985), and Jibson and Keefer (1989) and to the failure rate analysis technique used previously by Aniya (1985), Dikau (1990), and Henderson (1997) to investigate landslide distributions not associated with earthquakes.

To begin the discussion of the Loma Prieta analysis, Section 2 of this paper describes the setting and occurrence of the earthquake. Section 3 summarizes data on landslides generated by the earthquake. Section 4 presents the analysis and results, which are then discussed in Section 5.

2. Occurrence and setting of the Loma Prieta earthquake

The Loma Prieta earthquake occurred in the San Francisco Bay–Monterey Bay region of central California on October 17, 1989 (Fig. 1). The main shock had a Richter surface-wave magnitude (M_s) of 7.1 and a moment magnitude (**M**) of 6.9. The hypocenter was approximately 18 km deep at 37°02′ N, 121°53′ W, under the southern Santa Cruz Mountains, about 85 km southeast of San Francisco (Fig. 1; Plafker and Galloway, 1989; US Geological Survey Staff, 1990). Analyses of the aftershock distribution and geodetic modeling by several investigators resulted in slightly different interpretations of the fault rupture location and orientation, but most studies concluded that rupture occurred on the San Andreas Fault system, from a minimum depth of 3 km to a maximum depth of 18 km, on a steeply southwest-dipping plane (Plafker and Galloway, 1989; Lisowski et al., 1990; US Geological Survey Staff, 1990; Marshall et al., 1991; Snay et al., 1991; Wallace and Wallace, 1993; Williams et al., 1993; Árnadóttir and Segall, 1994). The fault rupture boundaries used in this analysis are taken from the modeling of Marshall et al. (1991), which shows the fault rupture as a rectangle, 34 km long and 5 km wide in plan view, with a dip of 60° SW, a depth ranging from 4 to 15 km, and a slip of 2.4 m right-lateral and 1.7 m reverse.

Much of the region affected by the earthquake is heavily urbanized, with a population of about 7 million people; even though the earthquake hypocenter was under a relatively sparsely populated part of that region, 62 people were killed and estimated damage was more than $6 billion (Plafker and Galloway, 1989). Landslides triggered by the earthquake killed one person, blocked numerous roads, and damaged or destroyed more than 100 residences and other structures (Keefer, 1998).

Topography in the region ranges from nearly flat bay margins, valley floors, and coastal terraces to the steep slopes of the California Coast Ranges and the near-vertical cliffs bordering the Pacific Ocean. The climate is classified as Mediterranean, characterized by warm, dry summers and cool, rainy winters. Mean annual precipitation varies throughout the region from about 250 to 2000 mm (Rantz, 1971). The earthquake occurred during the fourth year of a drought, when rainfall was only about 50 to 70% of normal, and at the end of the dry summer season — a combination of circumstances that made ground conditions especially dry. Most landslides generated by the earthquake were in the southern Santa Cruz Mountains, where the fault rupture was located (Fig. 1). Topography in this area ranges from gently rolling hills to steep, rugged ridges separated by narrow canyons, and elevations range from near sea level

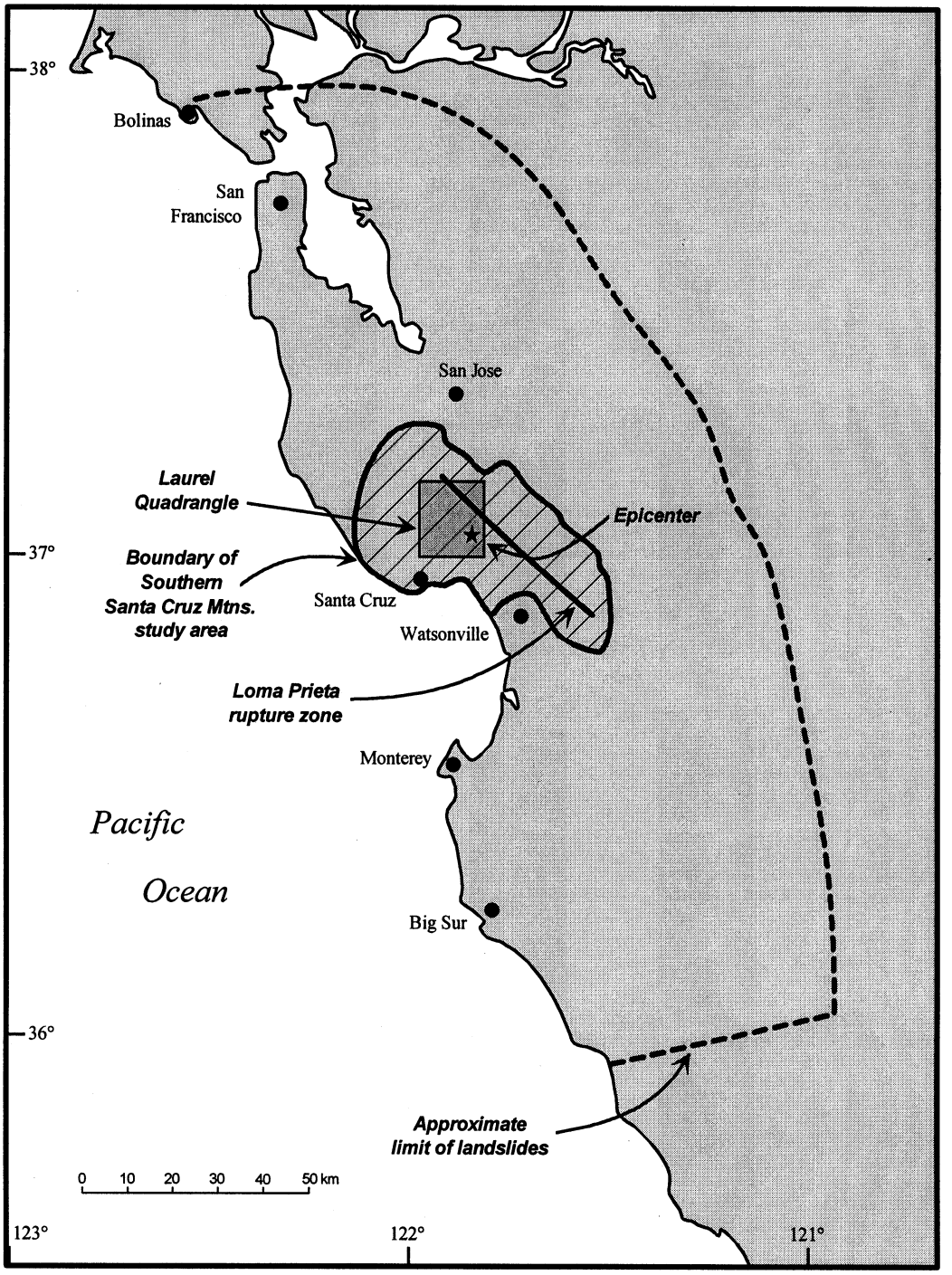

Fig. 1. San Francisco–Monterey Bay region of California, showing geographic limit of landslides generated by 1989 Loma Prieta earthquake, limits of southern Santa Cruz Mountains landslide area, earthquake epicenter (star), updip edge of fault rupture, and location of Laurel Quadrangle. After Keefer and Manson (1998).

to 1155 m asl. Dense redwood, oak-forest, or chaparral vegetation covers much of the area.

The largest part of the southern Santa Cruz Mountains is underlain by sedimentary rocks, which range in age from Upper Jurassic through Pliocene (McLaughlin et al., 1988, 1991; Brabb, 1989; Clark et al., 1989; Wentworth, 1993). Rock types include conglomerates, sandstones, siltstones, mudstones, and shales. These rocks are typically poorly or moderately indurated, structurally deformed by pervasive folding and local faulting, and covered by residual and colluvial soils as much as several meters deep. A large area northeast of the San Andreas Fault is underlain by rocks of the Upper Cretaceous to Lower Eocene? Franciscan Complex (McLaughlin et al., 1988, 1991; Wentworth, 1993); the predominant Franciscan rock type is a tectonic melange, composed of resistant blocks enclosed in a less resistant matrix of sheared argillite, tuff, and sandstone; other types of Franciscan rock include limestone, chert, basalt, and metasandstone. Franciscan rocks are typically more indurated but also more intensely fissured than the sedimentary rocks. Smaller areas of the southern Santa Cruz Mountains are underlain by typically well-indurated granitic rocks, schist, marble, serpentinite, basalt, and other mafic volcanics, and by unconsolidated to semiconsolidated Pliocene- through Holocene-aged sediments (McLaughlin et al., 1988, 1991; Brabb, 1989; Clark et al., 1989; Wentworth, 1993).

Prehistoric landslide deposits are widespread in this area (Cooper-Clark and Associates, 1975), and abundant landslides have occurred during historical times as a result of storms (Keefer et al., 1987; Ellen and Wieczorek, 1988) and previous earthquakes (Lawson, 1908; Youd and Hoose, 1978). Landslides associated with the 1906 San Francisco earthquake ($\mathbf{M} = 7.8$) were particularly numerous, and two large rock avalanches in the southern Santa Cruz mountains killed 10 people (Lawson, 1908; Youd and Hoose, 1978).

3. Landslides generated by the earthquake

The Loma Prieta earthquake produced landslides throughout an area of about 15,000 km^2 (Fig. 1). Observations from fixed-wing aircraft immediately after the earthquake, and preliminary examination of post-earthquake aerial photographs, showed that mapping the landslide distribution from the air was not feasible because of the dense vegetation cover in much of the affected region. Therefore, subsequent mapping and identification of landslides were conducted on the ground from traverses in vehicles and on foot. Initial ground-based investigation showed that most of the landslides had occurred in the southern Santa Cruz Mountains and along adjacent stretches of the coastal cliffs bordering the Pacific Ocean. Intensive mapping in those areas by more than 50 investigators subsequently identified a total of about 1280 earthquake-induced landslides throughout an area of approximately 2000 km^2 in the southern Santa Cruz Mountains (Weber and Nolan, 1989, 1992; Spittler and Harp, 1990; Keefer, 1991; Manson et al., 1992; Keefer et al., 1998; Keefer and Manson, 1998; Schuster et al., 1998). An additional 80 landslides occurred along adjacent coastal cliffs (Plant and Griggs, 1990; Griggs and Plant, 1998).

Outside these areas, reconnaissance-level field investigations indicated that the earthquake had generated an additional several dozen to possibly a few hundred landslides throughout the remaining 13,000 km^2 of the affected area; most of these latter landslides were small rock falls, rock slides, or soil slides with volumes less than 100 m^3 (Keefer and Manson, 1998). Landslides occurred as far as 133 km from the epicenter and 100 km from the fault rupture (Keefer and Manson, 1998; Fig. 1).

Using the landslide classifications of Keefer (1984a) and Keefer and Wilson (1989), 74% of the landslides in the southern Santa Cruz Mountains were classified as Category I landslides ('disrupted slides and falls'). Most of these were rock falls, rock slides, and disrupted soil slides, which ranged up to several thousand cubic meters in volume (Keefer and Manson, 1998). 26% of the landslides were classified as Category II, 'coherent slides'. These were rotational slumps and translational block slides, which had volumes ranging up to tens of millions of cubic meters (Keefer, 1991; Keefer and Manson, 1998; Keefer et al., 1998).

4. Analysis of landslide distribution

The statistical analysis of the landslide distribution was conducted for the landslides that occurred in the southern Santa Cruz Mountains, where the landslide concentration was highest and data were relatively complete. The analysis used localities of landslide sources recorded in Keefer and Manson (1998, plates 1 and 2). Some of the recorded landslide sources produced more than one landslide, but the analysis was not weighted to account for this, nor for differences in landslide volumes. The analysis was carried out using the digitally compiled geologic map of Wentworth (1993) and digital elevation models (DEMs) with 30 m × 30 m grid spacings produced from US Geological Survey 7.5′ (1:24,000 scale) topographic maps. Landslides in human-built fill and landslides produced by soil liquefaction, such as lateral spreads, were excluded from the analysis. Based on these criteria, the analysis was conducted for an area of 1920.41 km^2 that contained 1046 landslide sources (Fig. 2). Thus the average landslide concentration in the southern Santa Cruz Mountains was

$$LC_{average} = 1046/1920.41 \text{ km}^2$$

or

$$LC_{average} = 0.54 \text{ landslides/km}^2.$$

For comparison, the average landslide concentration throughout the rest of the area affected by the earthquake was at least an order of magnitude lower than that in the southern Santa Cruz Mountains, based on the occurrence of several dozen to a few hundred landslide sources throughout an area of about 13,000 km^2.

4.1. Variation of landslide concentration with distance from earthquake source

Variation of landslide concentration with distance was investigated using three different definitions of the earthquake source: the epicenter, the surface projection of the fault plane of Marshall et al. (1991), and the surface projection of the updip edge of that fault plane. For each analysis, LC was determined for a sequence of concentric bands 1 km wide extending outward from the source; the 1 km band width was selected after initial trial and error to provide sufficient detail for analysis while aggregating enough landslide sources within each band to yield a meaningful result. The outer bands were truncated where they intersected the boundary of the southern Santa Cruz Mountains area.

Fig. 3 shows the variation of LC with epicentral distance, r_e. LC values decrease from 13.37 landslides/km^2 at $r_e = 1$ km to less than 1 landslide/km^2 at distances greater than 10 km. Whereas little theoretical basis exists for choosing a particular functional form for an LC vs. r_e relation, the rapid decrease in LC with distance is well fit ($R^2 = 0.97$; $P \ll 0.001$) with the simple power law regression

$$LC = 14.675 r_e^{-1.3284}$$

where r_e is in kilometers and LC is in landslides per square kilometer.

Using surface projections of the fault plane and of its updip edge to define the earthquake source, the highest LC values are also adjacent to the source, with values decreasing rapidly as distances increase (Figs. 4 and 5). Again, with little theoretical basis for choosing a functional form, these data are fit best empirically with regression equations having an exponential form. For distances from the surface projection of the fault plane (Fig. 4)

$$LC = 1.061 \exp(-0.1582 r_p) \quad (R^2 = 0.80;\ P \ll 0.001)$$

and for distances from the surface projection of the updip edge of the fault plane (Fig. 5)

$$LC = 4.856 \exp(-0.3368 r_l) \quad (R^2 = 0.85;\ P \ll 0.001)$$

where LC is in landslides per square kilometer, r_p is the distance to the surface projection of the fault plane in kilometers, and r_l is the distance to the surface projection of the updip edge of the fault plane in kilometers.

These three definitions of the earthquake source, which neglect depth effects, were chosen for simplicity. Other definitions of the source that included depth effects, such as pseudo-depth (Boore et al., 1997) or hyper-depth terms (Abrahamson and Silva, 1997), would result in

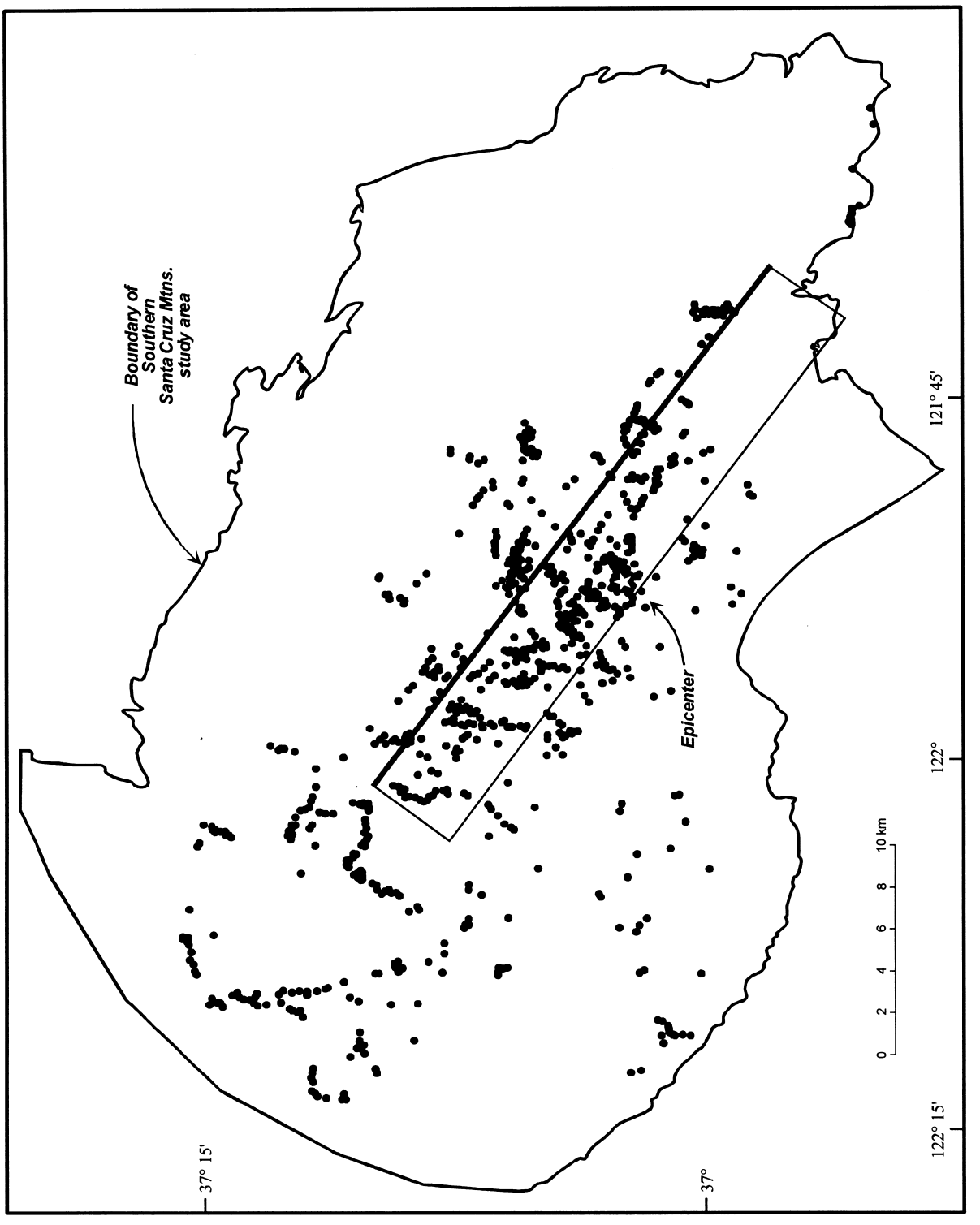

Fig. 2. Locations of earthquake-induced landslides (filled circles), epicenter, and surface projection of fault rupture defined by Marshall et al. (1991; rectangle with heavy line along updip edge) in the southern Santa Cruz Mountains.

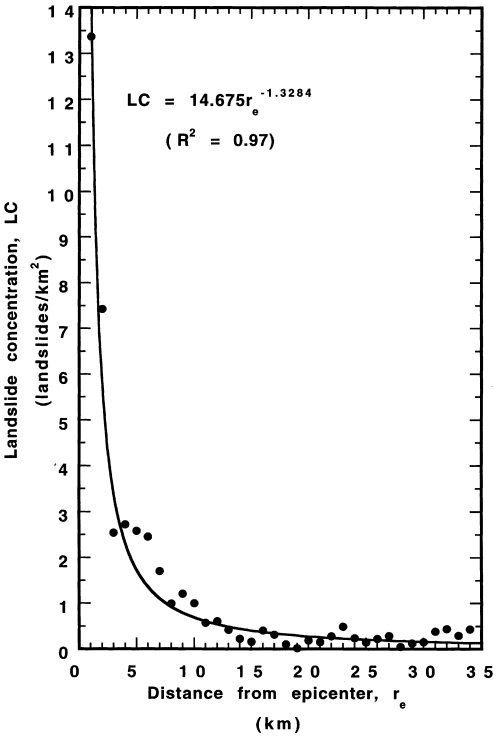

Fig. 3. Landslide concentration vs. distance from earthquake epicenter. Solid line is best-fit regression line, which has power law form.

different specific LC vs. distance relations and possibly different forms of the empirical best-fit regressions. However, regardless of the particular form of the relation, all measures of LC vs. distance from the source analyzed here show that the occurrence of landslides is strongly concentrated near the earthquake source. LC values above 0.54 landslides/km^2 (the average value for the southern Santa Cruz Mountains area) occur only at distances less than 12 km from the epicenter and 5 to 7 km from the surface projections of the fault rupture. In addition, for all three measures, LC values decrease rapidly with distance even within these short ranges (Figs. 3–5). The distances that encompass high LC values are especially short compared with the maximum distances of earthquake-induced landslides from the epicenter and fault rupture of this event — 133 and 100 km, respectively (Keefer and Manson, 1998).

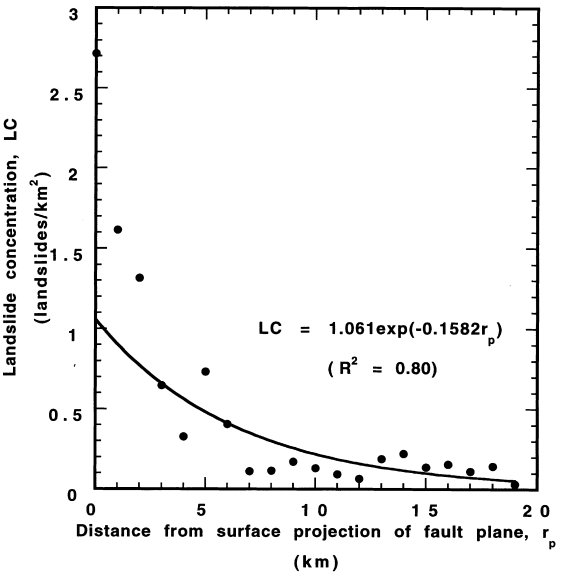

Fig. 4. Landslide concentration vs. distance from surface projection of fault plane defined by Marshall et al. (1991). Solid line is best-fit regression line, which has exponential form.

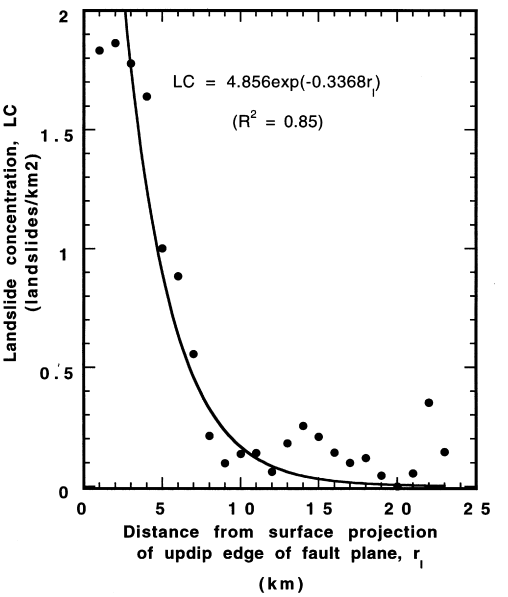

Fig. 5. Landslide concentration vs. distance from surface projection of updip edge of fault plane defined by Marshall et al. (1991). Solid line is best-fit regression line, which has exponential form.

4.2. Variation of landslide concentration with slope steepness

Within the area of the southern Santa Cruz Mountains, average slope steepness was calculated for each 30 m × 30 m DEM grid cell. For each 1° interval of slope steepness, the LC was calculated from determinations of the number of grid cells with that average slope steepness and the number of landslide sources present within those grid cells. For example, 64,111 grid cells have average slope steepness values between 10 and 11°. As each 30 m × 30 m grid cell has a surface area of 0.0009 km^2, these grid cells have an aggregate surface area of 57.70 km^2. They contain a total of 24 landslide sources, and so the landslide concentration is

$$LC_{\text{slope } 10^\circ} = 24 \text{ landslides}/57.70 \text{ km}^2$$

or

$$LC_{\text{slope } 10^\circ} = 0.42 \text{ landslides/km}^2.$$

Fig. 6 shows the percentage of the total surface area and percentage of landslide sources contained within each 1° interval of slope steepness, and

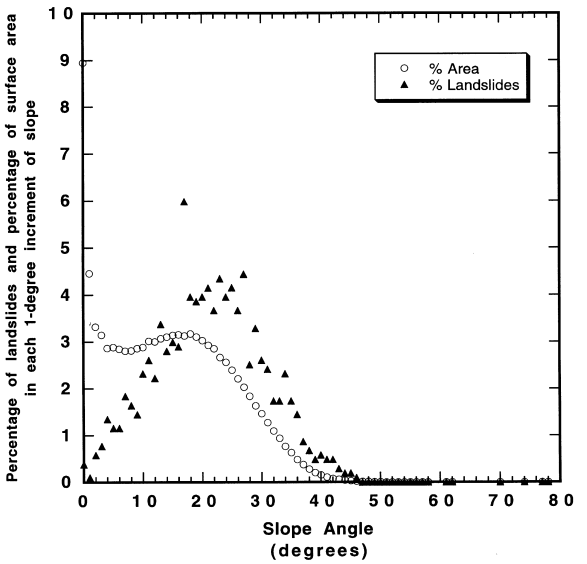

Fig. 6. Percentage of landslides and percentage of total surface area in southern Santa Cruz Mountains contained within each 1° interval of slope steepness, as calculated from digital elevation models with 30 m × 30 m grid cells.

Fig. 7 shows the landslide concentration in relation to the slope steepness. Average slopes for the grid cells range from 0 to 78°, and landslides occurred in grid cells with average slopes ranging from 0 to 46°. The absence of landslides from grid cells with steeper slopes is almost certainly due to the small number of such grid cells (Fig. 6), which together cover less than 0.03% of the total surface area. The occurrence of a few landslides in cells with slopes of less than 5° contrasts with previous findings (Keefer, 1984a), but is probably due to the averaging technique used to calculate slope in the DEMs, which masks short stretches of relatively steep slope that may occur within a 30 m × 30 m cell.

For grid cells with slopes between 0 and 47°, LC values increase rapidly with steepness; the increases are especially pronounced for slopes steeper than 34° (Fig. 7). The data are fit well empirically with two linear regression lines

$$LC = 1.5897 \tan\theta + 0.17045$$

$$(R^2 = 0.86;\ P \ll 0.001) \text{ for } \theta < 34^\circ$$

and

$$LC = 5.9033 \tan\theta$$

$$(R^2 = 0.71;\ P < 0.001) \text{ for } \theta \geq 34^\circ$$

where LC is in landslides per square kilometer, and θ is the angle of slope steepness. The data are also fit well by the single exponential regression (Fig. 7)

$$LC = 0.15159 \exp(3.2602 \tan\theta$$

$$(R^2 = 0.90;\ \theta < 47^\circ;\ P \ll 0.001).$$

4.3. Variation of landslide concentration with rock type

An LC value was determined for each geologic unit in the southern Santa Cruz Mountains that is shown on the map compiled by Wentworth (1993). Rocks underlying approximately one-quarter of this area were not assigned to named units and thus were not differentiated on the geologic map. Results for the rest of the area, underlain by 24 individual geologic units, are shown in Table 1 and Fig. 8. Individual units were grouped into six cate-

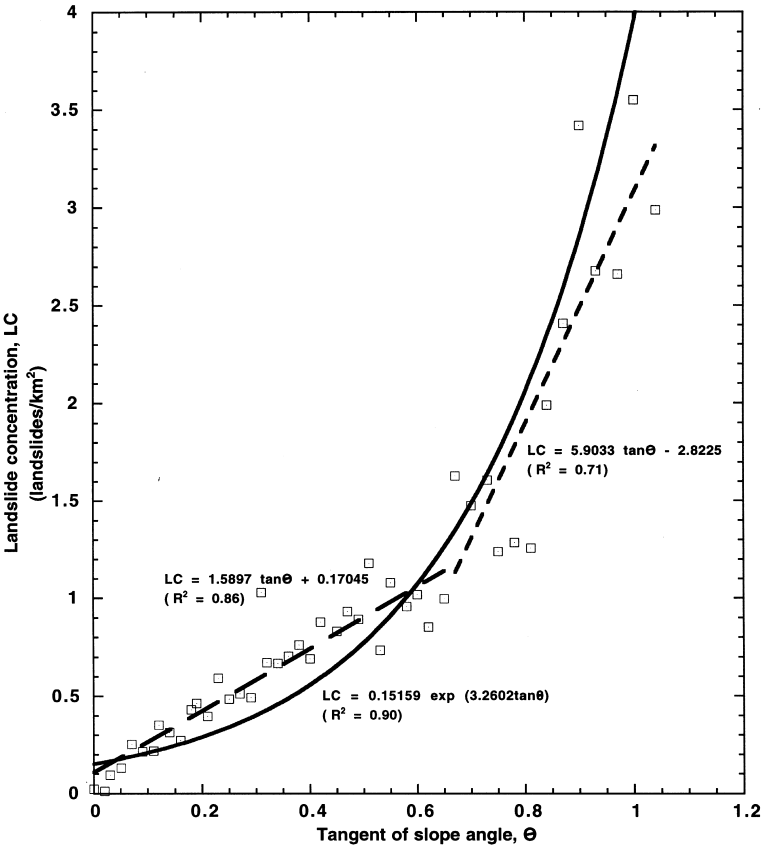

Fig. 7. Landslide concentration vs. slope inclination. Solid line is best-fit regression line for all slopes, which has exponential form. Long-dash line is best-fit linear regression line for slopes less than 34°; short-dash line is best-fit linear regression line for slopes steeper than 34°.

gories on the basis of lithology: (1) unconsolidated and semiconsolidated sediments of uppermost Tertiary through Holocene age; (2) weakly cemented sandstones and siltstones of the Pliocene Purisima Formation; (3) moderately indurated Tertiary formations consisting primarily of siltstone, mudstone, and shale; (4) moderately indurated Tertiary formations consisting primarily of sandstone; (5) the heterogeneous Great Valley Sequence, consisting of clastic sedimentary rocks of Jurassic through Cretaceous age; and (6) typically well-indurated igneous, metamorphic, and Franciscan Complex rocks.

With the exception of unconsolidated and semiconsolidated materials, which typically underlie gentle slopes [Table 1; Fig. 9(A)], LC values generally correlate with lithology. The Franciscan Complex, igneous, and metamorphic rocks all have low LC values, with a mean LC of 0.17 landslides/km^2 (Tables 1 and 2; Fig. 8). The moderately indurated Tertiary sandstones have a mean LC value of 0.56 landslides/km^2, whereas the finer-grained Tertiary units with moderate cementation have a mean LC value of 0.92 landslides/km^2. The LC value for the heterogeneous Great Valley Sequence is 0.77 landslides/km^2, intermediate between these means. The LC value of the weakly cemented Purisima Formation rocks is 2.03 landslides/km^2, the highest among all units. The unconsolidated and semiconsolidated units have relatively low LC values, with a mean of 0.21 landslides/km^2, almost certainly owing to the gentle slopes in most areas underlain by these units [Table 1; Fig. 9(A)]. A one-way analysis of vari-

Table 1
Geologic units, ages, predominant lithologies, mapped areas, median slopes, landslide concentrations, seismic slope-stability ratings, and shear strengths for geologic units in southern Santa Cruz Mountains[a]

Geologic unit	Age	Predominant lithology (after McLaughlin et al., 1988, 1991; Brabb, 1989; Clark et al., 1989)	Mapped area (km^2)	Landslide concentration (landslides/km^2)	Median slope angle (°)	Seismic slope-stability rating (after Wieczorek et al., 1985)	Mean effective friction angle (weighted) (°) (after McCrink and Real, 1996)	Group median cohesion (weighted) (kPa) (after McCrink and Real, 1996)	Number of shear strength tests (from McCrink and Real, 1996)	Effective strength at 3 m depth (kPa)
Holocene undivided	Q	Unconsolidated gravel, sand, silt, and clay	61	0.16	1	C*	29.6	25.4	66	58.8
Aromas Sand	Q	Aeolian sand and fluvial gravel, sand, silt, clay	47	0.40	9	B*	29.6	25.4	0#	58.8
Santa Clara Formation	QT	Coarse fluvial gravel and fanglomerate	33	0.06	10	C	nd	nd	nd	nd
Purisima Formation	T	Weakly consolidated sandstone and siltstone	187	2.03	15	C	33.1	25.2	79	63.5
Santa Cruz Mudstone	T	Laminated siliceous organic mudstone	91	0.21	17	C	29.5	25.4	0#	58.7
Monterey Formation	T	Flaggy, hard mudstone, porcelanite, and micaceous siltstone	34	0.49	15	C	29.5	25.4	2	58.7
Lambert Shale	T	Laminated organic mudstone, sandy siltstone, and sandstone	25	1.37	20	C	12.8	35.9	6	49.3
San Lorenzo Formation (undivided)	T	Carbonaceous shale, mudstone, and minor interbedded sandstone	26	1.24	18	C	27.4	25.4	0#	55.9
Rices Mudstone Member of San Lorenzo Formation	T	Mudstone and sandstone	45	1.37	17	C	34.9	27.0	35	68.0
Twobar Shale Member of San Lorenzo Formation	T	Laminated clay shale and mudstone	12	1.25	17	C	27.4	25.4	5	55.9
Locatelli Formation	T	Micaceous siltstone	4	0.52	13	C**	nd	nd	nd	nd
Santa Margarita Sandstone	T	Friable sandstone and conglomerate	52	0.21	10	B	36.0	23.9	0#	66.7
Temblor Sandstone	T	Friable to compact sandstone with minor mudstone and conglomerate	11	0.00	15	B**	nd	nd		nd
Lompico Sandstone	T	Arkosic and calcareous sandstone	21	0.94	14	A	36.0	23.9	5	66.7
Vaqueros Sandstone	T	Arkosic and glauconitic sandstone with interbeds of mudstone	140	0.94	20	A	33.3	24.3	22	62.9
Zayante Sandstone	T	Muddy sandstone, sandy siltstone, and conglomerate	8	0.39	18	A*	27.4	25.4	0#	55.9
Butano Sandstone	T	Sandstone with interbeds of siltstone and shale	94	0.90	19	A	28.9	26.2	26	58.7
Great Valley Sequence	KJ	Conglomerate, sandstone, mudstone, and shale	52	0.78	25	Variable	nd	nd	nd	nd
Franciscan Complex	TKJ	Melange-resistant blocks in matrix of sheared argillite, tuff, metasandstone, chert, and volcanic detritus, with local basalt, schist, and limestone	338	0.07	19	Variable	nd	nd	nd	nd
Mindego Basalt	T	Basalt	3	0.29	23	A	nd	nd	nd	nd
Granitic rocks	Mz	Granite, granodiorite, quartz monzonite, quartz diorite, and adamellite	97	0.18	16	A*	36.0	23.9	0##	66.7
Metasedimentary rocks	Mz	Pelitic schist, quartzite, and marble	26	0.15	11	A	29.5	25.4	0##	58.7
Mafic volcanics	Mz	Ultramafic cumulates, interlayered with gabbro	7	0.28	23	A*	36.0	23.9	0##	66.7
Serpentinite	Mz	Mildly to highly serpentinized ultramafic rocks	27	0.07	15	C	36.0	23.9	0##	66.7

[a] Age: Q signifies Quaternary; QT signifies Upper Tertiary through Quaternary; T signifies Tertiary; KJ signifies Jurassic through Cretaceous; TKJ signifies Jurassic through Tertiary; Mz signifies Mesozoic. Seismic slope-stability rating: A signifies strongest rocks; B signifies intermediate-strength rocks; C signifies weakest rocks. * Indicates rating by McCrink and Real (1996). ** Indicates rating by the author. No symbol indicates rating by Wieczorek et al. (1985). Effective strength at 3 m depth assumes dry conditions and unit weight of 2000 kg/m^3. nd Signifies no data. # indicates shear strength estimated from lithologic similarity to other, tested unit. ## indicates shear strength estimated from published values on materials with similar lithology.

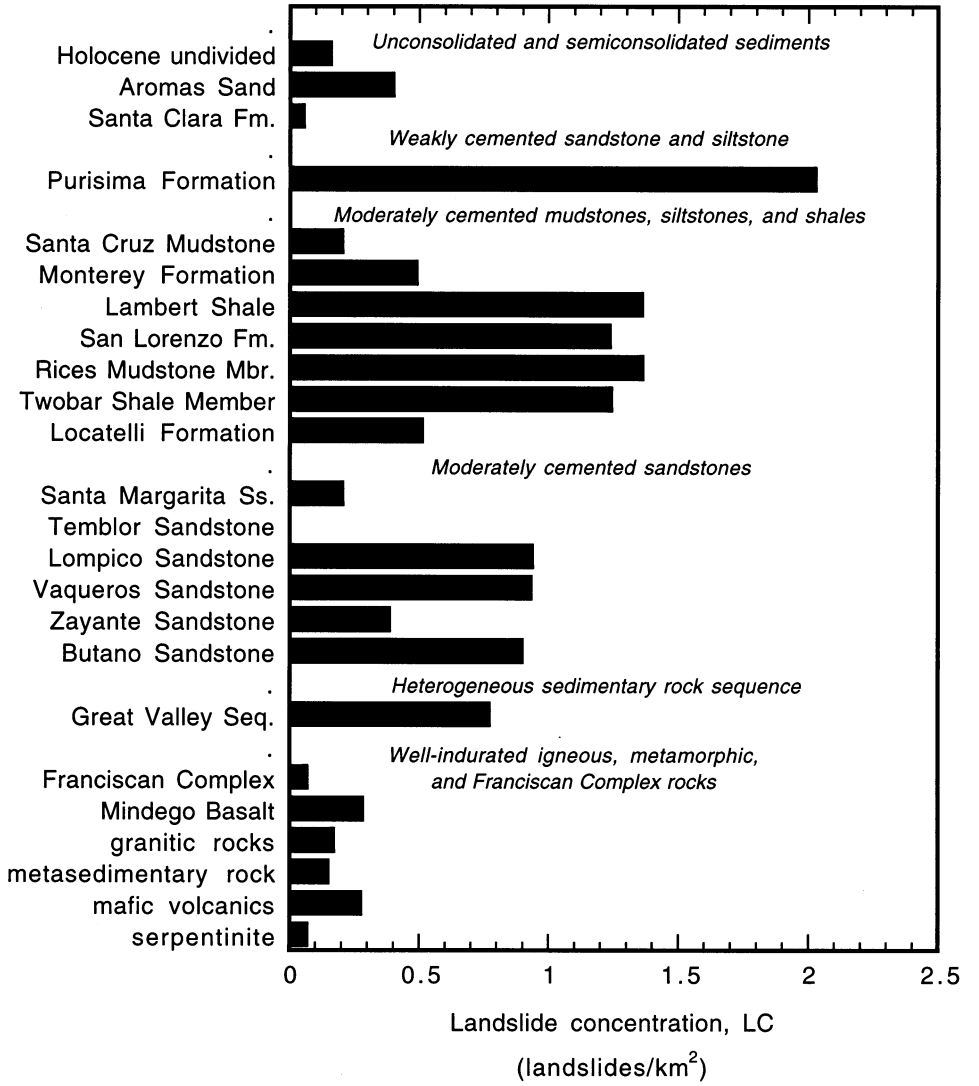

Fig. 8. Landslide concentrations for geologic units in the southern Santa Cruz Mountains.

ance (ANOVA) determination with Student's *t* tests was used to evaluate whether differences in mean LC values among lithologic groups are significant. The LC of the Purisima Formation is significantly higher than that of any other group formation, and the mean LC for the fine-grained Tertiary rocks is significantly higher than those of the Franciscan, igneous, and metamorphic rocks and of the unconsolidated and semiconsolidated sediments (Table 3).

The possibility that differences in slope steepness among units may have affected LC values was investigated by determining the distribution of slope steepness for each unit (Fig. 9). With a few exceptions, these distributions have similar shapes and ranges. The most prominent exception involves the unconsolidated and semiconsolidated sedimentary units, which have much lower slopes than the other units [Fig. 9(A)]. Most areas underlain by these units slope less than 10° (less

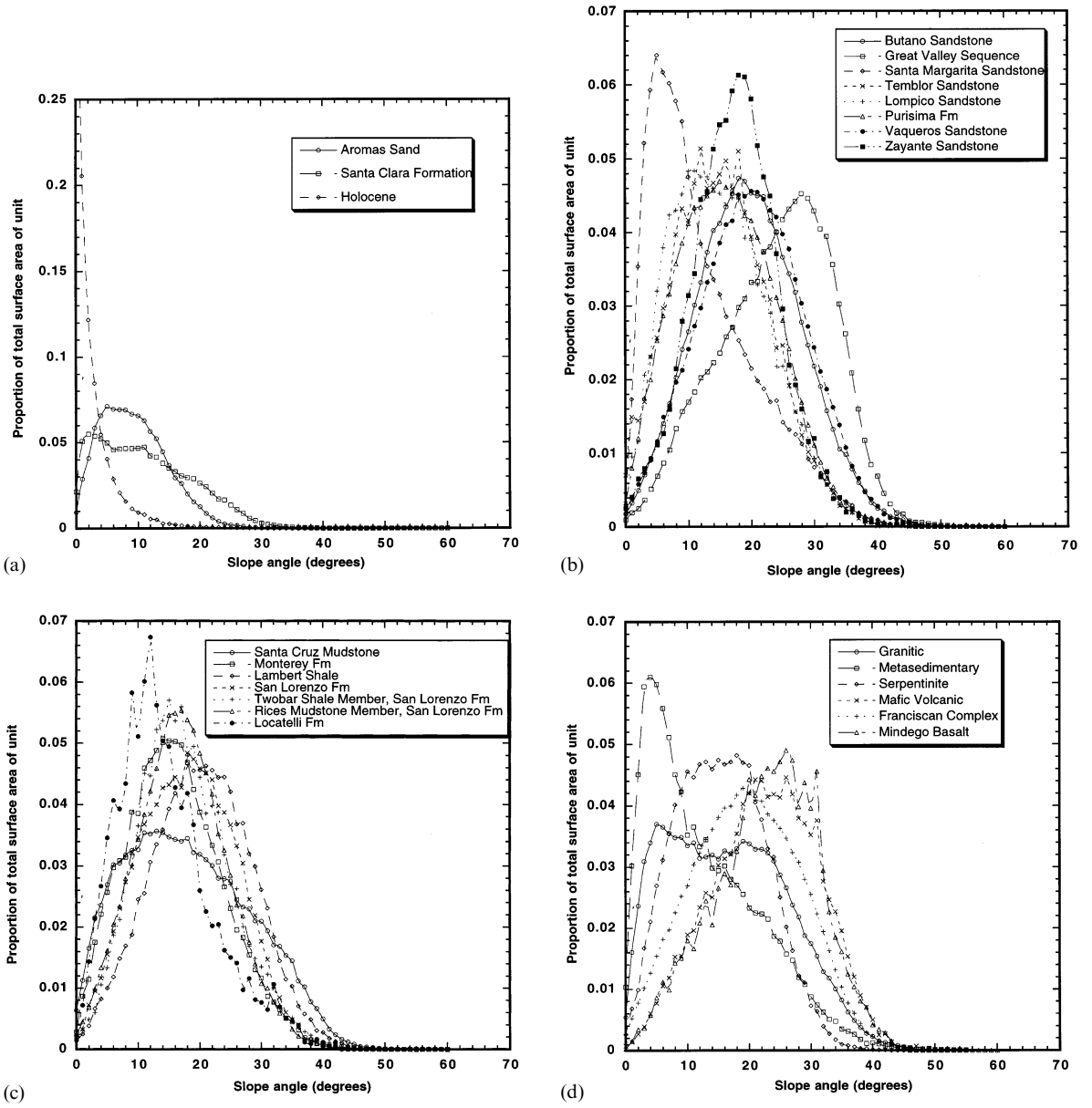

Fig. 9. Percentage of total surface area of each geologic unit in southern Santa Cruz Mountains contained within each 1° interval of slope steepness, as calculated from digital elevation models with 30 m × 30 m grid cells. (a) Unconsolidated and semiconsolidated sediments. (b) Purisima Formation, Great Valley Sequence, and moderately indurated Tertiary formations consisting primarily of sandstone. (c) Moderately indurated Tertiary formations consisting primarily of siltstone, mudstone, and shale. (d) Igneous, metamorphic, and Franciscan Complex rocks.

than 2° in the case of the Holocene undivided unit), and these low slopes are associated with low LC values (Table 1; Fig. 8). Other exceptions are the metasedimentary rocks [Fig. 9(D)], the Santa Margarita Sandstone [Fig. 9(B)], and possibly the Locatelli Formation [Fig. 9(C)], all of which are

Table 2
Mean values of landslide concentration for lithologic groups of rocks in the southern Santa Cruz Mountains

Lithologic group	Mean landslide concentration (landslides/km^2)	Standard error
Unconsolidated and semiconsolidated sediments	0.21	0.21
Weakly cemented sandstones and siltstones (Purisima Formation)	2.03	0.37
Moderately cemented mudstones, siltstones, and shales	0.92	0.14
Moderately cemented sandstones	0.56	0.15
Great Valley Sequence	0.78	0.37
Well-indurated igneous, metamorphic, and Franciscan Complex rocks	0.17	0.15

Table 3
Results of one way analysis of variance (ANOVA) tests comparing each pair of mean landslide concentration values for lithologic groups

	Student's t test values for comparison of mean landslide concentrations for lithologic groups. Positive values show pairs of means that are significantly different				
	Weakly cemented sandstones and siltstones (Purisima Formation)	Moderately cemented mudstones, siltstones, and shales	Moderately cemented sandstones	Great Valley Sequence	Well-indurated igneous, metamorphic, and Franciscan Complex rocks
Unconsolidated and semiconsolidated sediments	0.93	0.18	−0.19	−0.32	−0.51
Weakly cemented sandstones and siltstones (Purisima Formation)		0.29	0.63	0.16	1.02
Moderately cemented mudstones, siltstones, and shales			−0.07	−0.68	0.32
Moderately cemented sandstones				−0.62	−0.06
Great Valley Sequence					−0.23

associated with lower than average slopes, and the Great Valley Sequence, which forms relatively steep slopes [Fig. 9(D)]. However, these steeply sloping Great Valley Sequence rocks do not have a particularly high LC value (0.78 landslides/km^2). LC values of the Santa Margarita, Locatelli, and metasedimentary rocks are lower than the means for their respective lithologic groups, but in no case are minima (Table 1; Fig. 8). Thus, except for the unconsolidated and semiconsolidated sediments, the differences in LC among geologic units are evidently related to differences in slope steepness to only a small degree. The slope distributions may be represented relatively well by the simplified measure of median slope for each unit (Table 1). No statistically significant correlations were found relating LC to median slope using any regressions of simple functional form (linear, logarithmic, power law, and exponential; $R^2 < 0.08$ in all cases).

The possibility that LC values of individual units correlate with variations in distance to the earthquake source was also investigated; distances from the epicenter and surface projection of the updip edge of the fault plane to the centroid (center of mass) of each geologic unit were calculated and compared with the LC value for that unit. No statistically significant correlations were found relating LC to either measure of distance using regressions of linear, logarithmic, power law or exponential form ($R^2 < 0.07$ for all cases). Additional linear regressions were performed, weighting LC values with the mapped area of each unit. The weighted regression for epicentral dis-

tance was not statistically significant ($R^2=0.08$), but the weighted regression relating LC to distance from the surface projection of the updip edge of the fault rupture (Fig. 10) had marginal significance ($R^2=0.25$; $P=0.013$). Thus, differences in distance from the earthquake source to the areas underlain by various geologic units may account for a small part of the differences in LC values. However, except for the low slopes associated with areas of unconsolidated and semiconsolidated sediments, most of the differences among LC values of geologic units must be due to factors other than differences in slope or distance from the earthquake source.

Differences in material strength among geologic units are a likely source of some of the differences in LC values. Although tensile strength may be the most important strength parameter for some particularly steep slopes subjected to earthquake shaking (Sitar and Clough, 1983), strength is most typically characterized by the effective shear strength

$$\tau=(\sigma-u)\tan\phi'+c'$$

where τ is the effective shear strength across a potential failure surface, σ is the normal stress across that surface, u is the pore-water pressure acting on the failure surface, ϕ' is the effective angle of internal friction, and c' is the effective cohesion.

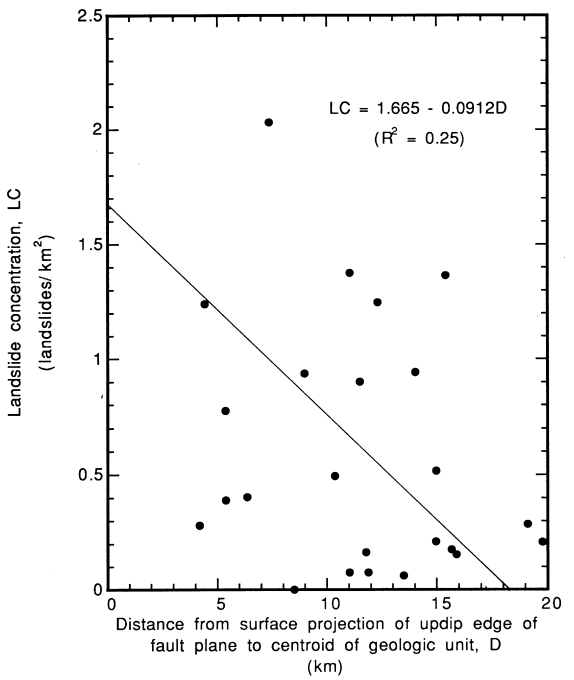

Fig. 10. Landslide concentrations associated with each geologic unit vs. distance between surface projection of updip edge of fault plane and centroid of unit. Solid line is best-fit linear regression line, with data weighted for mapped area of unit.

Many of the geologic units in the southern Santa Cruz Mountains were rated for seismic slope-stability hazard in an area immediately to the north by Wieczorek et al. (1985). For that hazard evaluation, the units were divided into three categories on the basis of estimated shear strength: (A) crystalline rocks and well-cemented sandstones (estimated effective friction angle $\phi'=35^\circ$ and estimated effective cohesion $c'=14.4$ kN/m^2); (B) unconsolidated and weakly cemented sandstones ($\phi'=35^\circ$, $c'=0$); and (C) shales and clays ($\phi'=20^\circ$, $c'=0$). Using the criteria established by Wieczorek et al. (1985), McCrink and Real (1996) rated several additional geologic units in the Laurel quadrangle area of the southern Santa Cruz Mountains, where many of the landslides triggered by the Loma Prieta earthquake occurred (Fig. 1), and I rated two additional units using these criteria (Table 1). Wieczorek et al. (1985) used combinations of the rock unit category and slope angle to rate susceptibility to seismic slope failure. Assuming a uniform distribution of slope inclinations among the various units, the strongest ('A') units should produce the lowest LC values, units of moderate strength ('B') intermediate LC values, and the weakest ('C') units the highest LC values.

Mean LC values for units in each of the three categories were calculated (Table 4), and ANOVA determinations with Student's t tests were to evaluate the significance of the differences in mean LC values among the categories. Analyses were performed for both the original set of units as rated by Wieczorek et al. (1985) and for the more extensive set of units that included those rated by McCrink and Real (1996) and by myself. Analyses were also performed for both the original and extensive sets of units after removing the six units associated with relatively low slopes (Holocene

Table 4
Mean values of landslide concentrations for rock categories rated using seismic slope-stability rating system of Wieczorek et al. (1985)[a]

Rock category	Original		Extensive	
	Mean landslide concentration (landslides/km^2)	Standard error	Mean landslide concentration (landslides/km^2)	Standard error
A	0.63	0.28	0.51	0.19
B	0.21	0.62	0.20	0.31
C	0.90	0.21	0.80	0.16
Excluding units with relatively low slopes (Holocene undivided, Aromas Sand, Santa Clara Formation, Santa Margarita Sandstone, Locatelli Formation, and metasedimentary rocks)				
A	0.77	0.30	0.56	0.21
B	nd	nd	0.00	0.55
C	1.00	0.21	1.00	0.19

[a] Original designates units rated by Wieczorek et al. (1985). Extensive also includes units rated by McCrink and Real (1996) and by the author. nd Signifies no data.

undivided, Aromas Sand, Santa Clara Formation, Santa Margarita Sandstone, Locatelli Formation, and metasedimentary rocks). No intermediate-strength (B) units were present in the original set after the units with relatively low slopes were removed; in this case the higher-strength (A) units had a lower mean LC than the lower-strength (C) units. For the other three cases, the intermediate-strength (B) unit or units had the lowest mean LC, whereas the strongest (A) units had intermediate mean LC values and the lowest-strength (C) units had the highest values (Table 4); ANOVA determinations indicate that none of the differences among means for any of the four sets of data are statistically significant.

McCrink and Real (1996) also undertook an extensive compilation of shear-strength data from the Laurel Quandrangle (Fig. 1). These data were obtained from geotechnical boring-logs, laboratory direct-shear test results, and geologic site investigations on file with the County of Santa Cruz Planning Department (McCrink and Real, 1996; McCrink, written communication, 1998). For each geologic unit, mean and median values of angle of internal friction, ϕ, and cohesion intercept, c, were reported (Table 1). In general, the investigators concluded that mean values of ϕ and median values of c for each formation or group of formations were most representative (Table 1), whereas in their best-case analysis of seismic slope-stability, they used mean values of ϕ for each unit and a value of $c=0$ everywhere.

To determine whether LC values correlate with the shear strength as compiled from these data, regression analyses were performed relating LC to two measures of shear strength: $\tan\phi$, and effective shear strength, τ, at a depth of 3 m, assuming dry conditions (pore-water pressure, $u=0$) and a uniform unit weight of 2000 kg/m^3. The depth of 3 m was chosen as the typical maximum depth for Category I landslides (Keefer, 1984a). Effective shear strength in this case is defined as

$$\tau = \gamma h \tan\phi + c$$

where γ is the unit weight (2000 kg/m^3) and h is the depth below the ground surface, measured perpendicular to the ground surface (3 m). For those units divided into fine- and coarse-grained components by McCrink and Real (1996), average values of ϕ and c, weighted for the number of tests performed on each component, were calculated for comparison with LC values. For both LC vs. $\tan\phi$ and LC vs. τ, regressions of linear, logarithmic, power law, and exponential form were performed, both including and excluding the six units associated with relatively low slopes. None of the regressions showed any statistically significant correlation between LC and the measure of shear strength employed, as for all cases $R^2<0.10$.

5. Discussion and conclusions

The method used herein to analyze the distribution of landslides from the Loma Prieta earthquake has advantages and limitations compared with other methods, such as multiple regression techniques or regional-scale slope-stability models. One advantage is the use of parameters that can be directly observed or measured and that are commonly recorded during comprehensive post-earthquake investigations: location of a landslide relative to the earthquake source, slope, and geologic unit in which a landslide occurs. A second advantage of this method is the ability to analyze each factor possibly affecting landslide distribution independently without assuming a priori any particular model or relationship between the factors. Yet another advantage is the ability to use different cell sizes for different parameters — for example, a fine 30 m × 30 m grid for slope and larger 1 km wide bands for distance from the earthquake source. In the case of the Loma Prieta earthquake, which produced about 1000 landslides in an area that contained more than one million 30 m × 30 m grid cells, the distance analysis would have produced meaningless results from the fine grid used in the analysis of slope effects. Conversely, using a grid much coarser than 30 m × 30 m would have rendered the analysis of slope effects equally meaningless. A major limitation of the method is the lack of explicit treatment of possible cross-correlation effects among the input parameters. In the case analyzed here, this limitation is due primarily to the differences in cell sizes used to analyze effects of slope, distance, and geologic unit. This limitation was partly compensated for by examining the slope inclinations associated with each geologic unit and by correlating the LC values of geologic units with distance from the centers of mass to the earthquake source.

Results of the analysis show that LC correlates inversely with all measures of distance from the earthquake source and positively with slope steepness. The correlations are strong with coefficients of determination, R^2, ranging from 0.80 to 0.97 for distance measures and from 0.71 to 0.90 for slope relations. The correlation between LC and epicentral distance has the highest coefficient of determination, $R^2 = 0.97$, suggesting that the seismic energy release that caused the landslides was concentrated near the epicenter rather than being uniformly distributed along the fault rupture. The specific relation between LC and slope is almost certainly affected by the size of the grid cell used in the analysis (30 m × 30 m), as the slope is averaged over each grid cell, thus masking the effects of short stretches of steeper than average slope, which may contain the actual landslide source. Thus the apparent occurrence of some landslides on slopes of only 1, 2, or 3°, for example, may be an artifact of the way in which this analysis was conducted; using DEMs with smaller grid sizes would almost certainly reduce this effect, at least down to the limit of resolution in landslide location and in the topographic mapping on which the DEMs are based. In any case, the strong correlations of LC with source distance and with slope indicate that, for this earthquake, landslide hazard was strongly concentrated on steep slopes close to the seismic source.

Correlation of LC with geologic unit is more complex. Variations in LC values among the geologic units were examined by grouping the units according to descriptions of lithology, and by attempting to correlate LC with shear strengths as measured or estimated by two different studies. The only statistically significant relations were those between LC values and the descriptions of lithology. The best-indurated materials (igneous, metamorphic, and Franciscan Complex rocks) had the lowest mean value of LC, which was significantly lower than means for weakly or moderately indurated sedimentary rocks. By contrast, the LC value of the relatively weakly cemented Purisima Formation was significantly higher than LC values of any other lithologic group. Moderately indurated sedimentary rocks in general had intermediate values of LC, with the mean LC value for units dominated by sandstones being lower than the mean for units where finer-grained rocks predominate. The unconsolidated and semiconsolidated units in the region, consisting of relatively young alluvium and other sediments, had anomalously low LC values, but this anomaly was almost certainly due to the relatively gentle slopes associated with these units.

No correlations were found between LC values and estimates or measurements of shear strength as averaged for each geologic unit. This lack of correlation is probably due to several factors. First, shear strength acts in combination with other such factors as slope, pore-water pressure, and the characteristics of ground motion on a local, site-specific basis; thus the influence of shear strength on landslide occurrence is almost certainly more complex than can be revealed by the analysis presented here, which is based on LC values determined for areas relatively large compared with individual landslide sources. Second, the shear strength values determined from the existing studies are averaged for each geologic unit, whereas shear strength varies substantially both laterally and with depth, particularly for geologic units as heterogeneous as most of those in the southern Santa Cruz Mountains area. Third, a uniform depth to failure surfaces was assumed in this analysis, whereas landslide depths varied from location to location. Finally, the effects of pore-water pressure were neglected and, while the area was unusually dry at the time of the earthquake, ground-water levels may have been high enough to influence slope-stability in at least a few localities (Keefer et al., 1998). These limitations in the use of shear-strength data, combined with the better correlations relating LC to descriptions of lithology, suggest that for regional-scale analyses of seismic landslide hazard, variations in hazard level might be better correlated with these lithologic descriptions than with measurements of shear strength.

In the southern Santa Cruz Mountains where the Loma Prieta earthquake produced most landslides, therefore, the landslide hazard was related strongly to slope and distance to the source and in a somewhat less certain way to lithology. Similar analyses of landslide distributions from other earthquakes are needed to better determine the forms and coefficients of relations that may be used to quantify earthquake-induced landslide hazards in various regions. Results of this study suggest that this hazard may be defined by using such readily determined characteristics as slope, distance from a potential source, and rock type.

Acknowledgements

I thank Sarah Christian, Monique Jaasma, and Scott Miles for GIS processing of the data; John Boatwright, Randall Jibson, Floriana Pergalani, Janusz Wasowski, Raymond Wilson, and an anonymous reviewer for thoughtful comments; and Carol Harden for bringing the failure rate analysis method to my attention.

References

Abrahamson, N.A., Silva, W.J., 1997. Empirical response spectral attenuation relations for shallow crustal earthquakes. Seismol. Res. Lett. 68, 94–127.

Aniya, M., 1985. Landslide-susceptibility mapping in the Amahata River Basin, Japan. Ann. Assoc. Am. Geogr. 75, 102–114.

Árnadóttir, T., Segall, P., 1994. The 1989 Loma Prieta earthquake imaged from inversion of geodetic data. J. Geophys. Res. 99, 21,835–21,855.

Boore, D.M., Joyner, W.B., Fumal, T.E., 1997. Equations for estimating horizontal response spectra and peak acceleration from western North America earthquakes: a summary of recent work. Seismol. Res. Lett. 68, 128–153.

Brabb, E.E., 1989. Geologic map of Santa Cruz County, California. US Geological Survey Miscellaneous Investigations Series Map I-1905, scale 1:62,500.

Clark, J.C., Brabb, E.E., McLaughlin, R.J., 1989. Geologic map and structure sections of the Laurel 7-1/2′ Quadrangle, Santa Clara and Santa Cruz Counties, California. US Geological Survey Open-File Map 89-676, scale 1:24,000, two sheets, 31 pp.

Cooper-Clark and Associates, 1975. Preliminary map of landslide deposits in Santa Cruz County, California. In: Seismic Safety Element, Santa Cruz, California. Santa Cruz County Planning Department, scale 1:62,500.

Dikau, R., 1990. Derivatives from detailed geoscientific maps using computer methods. Z. Geomorph. 80, Suppl., 45–55.

Ellen, S.D., Wieczorek, G.F. (Eds.), Landslides, floods, and marine effects of the storm of January 3–5, 1982, in the San Francisco Bay region, California. US Geol. Survey Prof. Paper 1434 1988. 310 pp.

Griggs, G.B., Plant, N., 1998. Coastal-bluff failures in northern Monterey Bay induced by the earthquake. In: Keefer, D.K. (Ed.), The Loma Prieta, California earthquake of October 17, 1989 — landslides, US Geol. Survey Prof. Paper 1551-C, C33–C50.

Hansen, A., Franks, C.A.M., 1991. Characterisation and mapping of earthquake triggered landslides for seismic zonation, Proc. 4th Int. Conf. on Seismic Zonation, Stanford, CA Vol. 1., 149–195.

Henderson, J.P., 1997. Debris slides on Mount Leconte,

Tennessee, Abstr. 93rd Annual Meet. Association of American Geographers, Fort Worth, TX, 112.
Jibson, R.W., 1985. Landslides caused by the 1811–12 New Madrid Earthquakes. Ph.D. Dissertation, Stanford University, Stanford, CA, 232 pp.
Jibson, R.W., Keefer, D.K., 1989. Statistical analysis of factors affecting landslide distribution in the New Madrid seismic zone, Tennessee and Kentucky. Eng. Geol. 27, 509–542.
Keefer, D.K., 1984a. Landslides caused by earthquakes. Geol. Soc. Am. Bull. 95, 406–421.
Keefer, D.K., 1984b. Rock avalanches caused by earthquakes: source characteristics. Science 223, 1288–1290.
Keefer, D.K. (Ed.), 1991. Geologic hazards in the Summit Ridge area of the Santa Cruz Mountains, Santa Cruz County, California, evaluated in response to the October 17, 1989 Loma Prieta earthquake: report of the Technical Advisory Group. US Geol. Survey Open-File Rep. 91-618, 427 pp.
Keefer, D.K., 1993. The susceptibility of rock slopes to earthquake-induced failure (Technical Note). Bull. Assoc. Eng. Geol. 30, 353–361.
Keefer, D.K. (Ed.), 1998. The Loma Prieta, California earthquake of October 17, 1989 — landslides. US Geol. Survey Prof. Paper 1551-C, 185 pp.
Keefer, D.K., 1999. Earthquake-induced landslides and their effects on alluvial fans. J. Sediment. Res. 69, 84–104.
Keefer, D.K., Manson, M.W., 1998. Regional distribution and characteristics of landslides generated by the earthquake. In: Keefer, D.K. (Ed.), The Loma Prieta, California earthquake of October 17, 1989 — landslides, US Geol. Survey Prof. Paper 1551-C, C7–C32.
Keefer, D.K., Wilson, R.C., 1989. Predicting earthquake-induced landslides, with emphasis on arid and semi-arid environments. In: Sadler, P.M., Morton, D.M. (Eds.), Landslides in a semi-arid environment with emphasis on the Inland Valleys of Southern California, Inland Geological Society of Southern California Publications Vol. 2, Part 1. Inland Geological Society of Southern California, Riverside, CA, pp. 118–149.
Keefer, D.K., Wilson, R.C., Mark, R.K., Brabb, E.E., Brown III, W.M., Ellen, S.D., Harp, E.L., Wieczorek, G.F., Alger, C.S., Zatkin, R.S., 1987. Real-time landslide warning during heavy rainfall. Science 238, 921–925.
Keefer, D.K., Griggs, G.B., Harp, E.L., 1998. Large landslides near the San Andreas Fault in the Summit Ridge area of the Santa Cruz Mountains, California. In: Keefer, D.K. (Ed.), The Loma Prieta, California earthquake of October 17, 1989 — landslides, US Geol. Survey Prof. Paper 1551-C, C71–C128.
Lawson A.C., (Chairman), 1908. The California earthquake of April 18, 1906: report of the State Earthquake Investigation Commission. Carnegie Institution of Washington Publication 87. two volumes.
Lisowski, M., Prescott, W.H., Savage, J.C., Johnston, M.J., 1990. Geodetic estimate of coseismic slip during the 1989 Loma Prieta, California earthquake. Geophys. Res. Lett. 17, 1437–1440.
Manson, M.W., Keefer, D.K., McKittrick, M.A., 1992. Landslides and other geologic features in the Santa Cruz Mountains, California, resulting from the Loma Prieta earthquake of October 17, 1989. California Div. Mines Geol. Open-File Rep. 91-08 45 pp.
Marshall, G.A., Stein, R.S., Thatcher, W., 1991. Faulting geometry and slip from coseismic elevation changes; the 18 October, 1989 Loma Prieta, California earthquake. Seismol. Soc. Am. Bull. 81, 1660–1693.
McCrink, T.P., Real, C.R., 1996. Evaluation of the Newmark method for mapping earthquake-induced landslide hazards in the Laurel 7.5′ Quadrangle, Santa Cruz County, California. Final Technical Report to the US Geological Survey, Award No. 1434-93-G 2334, 32 pp.
McLaughlin, R.J., Clark, J.C., Brabb, E.E., 1988. Geologic map and structure sections of the Loma Prieta 7-1/2′ Quadrangle, Santa Clara and Santa Cruz Counties, California. US Geological Survey Open-File Map 88-752, scale 1:24,000, two sheets, 32 pp.
McLaughlin, R.J., Clark, J.C., Brabb, E.E., Helley, E.J., 1991. Geologic map and structure sections of the Los Gatos 7-1/2′ Quadrangle, Santa Clara and Santa Cruz Counties, California. US Geological Survey Open-File Report 91-593, scale 1:24,000, three sheets, 48 pp.
Plafker, G., Galloway, J.P (Eds.), Lessons learned from the Loma Prieta, California earthquake of October 17, 1989. US Geol. Survey Circ. 1045 1989. 48 pp.
Plant, N., Griggs, G.B., 1990. Coastal landslides caused by the October 17, 1989 earthquake Santa Cruz County, California. California Geol. 43, 75–84.
Rantz, S.E., 1971. Mean annual precipitation and precipitation depth–duration–frequency data for the San Francisco Bay region, California. US Geol. Survey Open-File Rep.. 23 pp.
Schuster, R.S., Wieczorek, G.F., Hope II, D.G., 1998. Landslide dams in Santa Cruz County, California, resulting from the earthquake. In: Keefer, D.K. (Ed.), The Loma Prieta, California earthquake of October 17, 1989 — landslides, US Geol. Survey Prof. Paper 1551-C, C51–C70.
Simonett, D.S., 1967. Landslide distribution and earthquakes in the Bewani and Torricelli Mountains New Guinea — a statistical analysis. In: Jennings, J.N., Mabbutt, J.A. (Eds.), Landform Studies from Australia and New Guinea. Cambridge University Press, Cambridge, pp. 64–84.
Sitar, N., Clough, G.W., 1983. Seismic response of steep slopes in cemented soils. Am. Soc. Civil Eng. J. Geotech. Eng. 109, 210–227.
Snay, R.A., Neugebauer, H.C., Prescott, W.H., 1991. Horizontal deformation associated with the Loma Prieta earthquake. Seismol. Soc. Am. Bull. 81, 1647–1659.
Spittler, T.E., Harp, E.L. (Compilers), 1990. Preliminary map of landslide features and coseismic fissures in the Summit Road area of the Santa Cruz Mountains triggered by the Loma Prieta earthquake of October 17, 1989. US Geological Survey Open-File Report 90-688, scale 1:4800, three sheets, 31 pp.
US Geological Survey Staff, 1990. The Loma Prieta, California earthquake: an anticipated event. Science 274, 286–293.

Wallace, M.H., Wallace, T.C., 1993. The paradox of the Loma Prieta earthquake: why did rupture terminate at depth? J. Geophys. Res. 98, 19,859–19,867.

Wang, W., Xu, B., 1984. Brief introduction of landslides in loess in China, Proc. 4th Int. Symp. on Landslides, Toronto Vol. 1., 197–207.

Weber, G.E., Nolan, J.M., 1989. Landslides and associated ground failure in the epicentral region of the October 17, 1989 Loma Prieta earthquake. Final Technical Report to US Geological Survey under Contract 14-08-0001-G 1861, 26 pp.

Weber, G.E., Nolan, J.M., 1992. Landslides in the epicentral region of the October 17, 1989 Loma Prieta earthquake — factors affecting the distribution of seismically induced landsliding, Proc. 35th Annual Meet. Association of Engineering Geologists, Los Angeles 33., 176–186.

Wentworth, C.M., (Compiler), 1993. General distribution of geologic materials in the southern San Francisco Bay region, California: a digital map database. US Geol. Survey Open-File Rep. 93-693 12 pp.

Wieczorek, G.F., Wilson, R.C., Harp, E.L., 1985. Map showing slope-stability during earthquakes in San Mateo County, California. US Geological Survey Miscellaneous Investigations Series Map I-1257-E, scale 1:62,500.

Williams, C.R., Árnadóttir, T., Segall, P., 1993. Coseismic deformation and dislocation models of the 1989 Loma Prieta earthquake derived from global positioning system measurements. J. Geophys. Res. 98, 4567–4578.

Wilson, R.C., Keefer, D.K., 1985. Predicting areal limits of earthquake-induced landsliding. In: Ziony, J. (Ed.), Earthquake hazards in the Los Angeles region — an earth-science perspective, US Geol. Survey Prof. Paper 1360, 317–345.

Youd, T.L., Hoose, S.N., 1978. Historic ground failures in northern California triggered by earthquakes. US Geol. Survey Prof. Paper 993 177 pp.